Int. J. Heat Mass Transfer. Vol. 11, pp. 1637–1652. Pergamon Press 1968. Printed in Great Britain

FLOW ABOUT A GROWING SPHERE IN CONTACT WITH A PLANE SURFACE

C. P. WITZE†, V. E. SCHROCK‡ and P. L. CHAMBRÉ§

(*Received* 25 *August* 1967 *and in revised form* 29 *April* 1968)

Abstract—A solution is presented describing the potential flow pattern in a semi infinite liquid surrounding a sphere that is growing while remaining tangent to a plane solid surface. An exact integral representation of the solution for the potential distribution is given. A simple analytic representation for the integrand was chosen to replace the exact form and thus provide closed form analytic results for both the potential and velocity distribution.

Properties of the flow field are examined. The total kinetic energy of the fluid agrees well with the result of an earlier but less detailed calculation by Shiffman and Friedman. For one specific g;owth law the pr*Is*-sure distribution was evaluated and used to form a new criterion for detachment of the sphere from the surface. The solution should find application in boiling bubble dynamics, underwater explosions and cavitation studies.

NOMENCLATURE

A,	surface area;
$A(q)$,	weighting function in equation (21);
a_i, b_i, B_i,	constants, defined in text;
F,	force;
g,	gravitational constant;
J_0,	ordinary Bessel function first kind, zero order;
p,	pressure;
q,	eigen values defined in equation (19);
R,	bubble radius;
$\dot{R}$,	$= \mathrm{d}R/\mathrm{d}t$;
R_s,	radius of sphere in tangent–sphere coordinates;
R_t,	radius of torus in tangent–sphere coordinates;
r,	coordinate define in Fig. 1;
r^*,	$= r/R$;
T,	kinetic energy of liquid;
T^*,	dimensionless kinetic energy, $= T/\rho_l \dot{R}^2 R^3$;
t,	time;
V,	velocity;
$V_\mu, V_\nu, V_r, V_\theta$,	velocity components in μ, ν, r, θ directions.

Greek symbols

α,	separation constant in equation (18);
β,	constant in bubble growth law $R = \beta t^{\frac{1}{2}}$;
ϕ,	velocity potential;
φ,	angular coordinate defined in Fig. 1;
ϕ^*,	dimensionless velocity potential, $\phi/2R\dot{R}$;
μ, ν,	coordinates in tangent–sphere system, Fig. 2;
μ^*,	dimensionless coordinate, $= 2R\mu$;
ν^*,	dimensionless coordinate, $= 2R\nu$;
ρ_l,	liquid density;
ρ_g,	vapor density;
θ,	angular coordinate defined in Fig. 1.

† Department of Nuclear Engineering, University of California, Berkeley, U.S.A.; formerly Nuclear Science and Engineering Fellow. Present address: Bellcomm, Inc., Washington, D.C., U.S.A.

‡ Department of Nuclear Engineering, University of California, Berkeley, U.S.A. This work was supported in part by USAEC Contract AT(11-1)-34, Project 42.

§ Department of Mathematics and Department of Nuclear Engineering, University of California, Berkeley, U.S.A. This work was supported in part by Contract Nonr-222(95).

INTRODUCTION

THE NATURE of the flow field in a semi infinite liquid about an expanding sphere that remains in contact with a plane solid wall is of relevance to a number of practical applications. In the theory of boiling bubble dynamics at a heated surface, for example, a hemispherical cavity in a semi-infinite fluid has usually been assumed as a first approximation. With the neglect of viscous forces such a geometric model leads to the trivial result of a spherically symmetric fluid flow field. Experiments have shown that bubbles in surface boiling rarely grow either as perfect hemispheres or spheres but with a range of shapes between these two extremes. The actual shapes appear too complicated for analysis at this time. A complete spherical geometry offers the possibility of studying certain asymmetric aspects of boiling bubble dynamics not revealed by the hemispherical geometry. A potential flow model (i.e. liquid is incompressible, inviscid and irrotational will be assumed because it offers the simplest means of investigating the general nature of the flow field without regard to the additional complexities of viscous effects which are especially important in the vicinity of the solid wall.

The only other known attempt in the literature to examine asymmetric fluid flow about an expanding cavity at a solid wall was a recent study by Kotake [1], who investigated the potential flow field about a truncated sphere. Detailed discussion concerning the flow patterns associated with this geometry was not presented however. In addition, the velocity potential obtained by solution to Laplace's equation did not satisfy the original boundary conditions for the problem nor did it predict the spherically symmetric result when the geometry was reduced to its limiting form as a hemisphere. In any event, the use of a spherical model for the expanding bubble offers the advantage that the effect of the wall on the flow field is maximized. Any other geometry between a sphere and a hemisphere offers a less pronounced effect on fluid dynamic asymmetry especially when viscous effects at the wall are neglected.

In previous studies of the growth of spherical cavities near a solid plane boundary the method of sources and image sinks has been employed [2]. When the sphere is assumed in contact with the surface this method is not convenient because it requires a very complex selection of point and line sources and sinks. The previous solution methods also give the total fluid kinetic energy without detailed knowledge of the flow field. For the application of the flow solution to the analysis of the dynamics of boiling bubble growth it is necessary to know the flow field in detail.

In this application the hydrodynamics are assumed uncoupled from the energy equation, i.e. heat diffusion to the interface (evaporation) controls the bubble growth rate. This is the same assumption made in other "asymptotic" boiling bubble growth solutions [3–5]. It should be noted that although the flow solution may be achieved without use of the energy equation the *magnitude* of velocities does depend upon the solution of the energy equation inasmuch as it determines the bubble surface velocity and, of course, the flow velocity is needed for the convective term in the energy equation. The rate of bubble growth is however assumed independent of the momentum equation. This is done by specifying the bubble surface velocity (from the separate solution of the energy equation) rather than specifying the pressure inside the bubble. In this regard the present solution has the same restriction as does the spherically symmetric result used in other analyses [3–5].

The equation to be solved in the liquid for the bounded velocity potential ϕ is Laplace's equation,

$$\nabla^2\phi = 0 \tag{1}$$

for the geometry shown in Fig. 1.

Recognizing the polar symmetry of the problem, the second order equation in two spatial variables requires the following boundary conditions (origin of coordinates at 0).

$$\frac{\partial \phi}{\partial \theta} = 0, \qquad \theta = 0; \quad 2R \leqslant r \leqslant \infty \tag{2a}$$

$$\frac{\partial \phi}{\partial n} = 0 \text{ on the solid wall} \tag{2b}$$

$$-\frac{\partial \phi}{\partial n} = \dot{R}(1 + \cos 2\theta) \text{ on the bubble surface} \tag{2c}$$

$$\frac{\partial \phi}{\partial r} = \frac{\partial \phi}{\partial \theta} = 0, r \to \infty; 0 \leqslant \theta \leqslant \frac{\pi}{2}. \tag{2d}$$

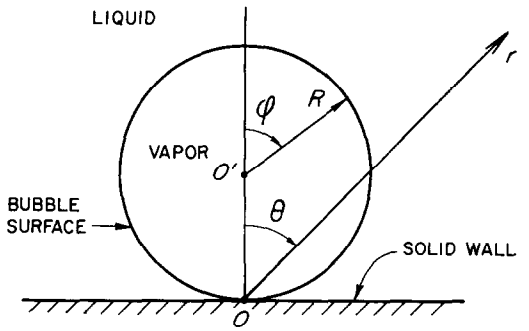

FIG. 1. Geometry for spherical bubble on plane wall.

Equation (2a) is a symmetry condition about the axis $\theta = 0$ and indicates that the flow is purely radial for $\theta = 0$ and all values of $r \geqslant 2R$. Boundary condition (2b) states that the normal component of the fluid velocity at the wall is zero, i.e. no fluid crosses the solid wall. The third boundary condition (2c) relates the normal gradient of the velocity potential at the bubble wall to the known normal component of the bubble surface velocity. The final condition (2d) states that the fluid velocity approaches zero very far away from the bubble. Inasmuch as the potential has an arbitrary datum and tends to a constant value we choose $\phi = 0$ as $r \to \infty$ to replace this condition. This changes the problem from a boundary value problem of the Neumann type to a mixed boundary value problem of the Dirichlet–Neumann type.

It should be noted that equation (1) is valid in transient incompressible flow which has been assumed for the present problem. In this case the entire flow field outside the sphere adjusts instantaneously to changes in the boundary condition (2c).

METHOD OF SOLUTION

Since, as indicated in the introduction, the method of images is not adaptable to the present geometry other methods were explored.

Separation of variables, which is successful for many problems involving Laplace's equation, requires that the physical boundaries of the region of applicability coincide with the coordinate surfaces of the system. In the description of the problem presented in the introduction (the $r - \theta$ coordinate system) Laplace's equation is separable and the conditions (2a, 2b, 2d) are simple descriptions on the coordinate surfaces. However a solution cannot be obtained in this geometry because the condition (2c) on the bubble surface is too complex, i.e. the prescribed gradient of the potential is not in the direction of one of the coordinates. Moving the origin of the coordinate system to the centre of the bubble O' alleviates the problem insofar as the bubble boundary condition is concerned but then a similar complication arises on the solid surface and at large distances from the bubble.

Fortunately a coordinate system exists which is compatible with the present problem. It is the "tangent–sphere coordinate system" whose properties are summarized, for example, by Moon and Spencer [6]. It is a member of a general class of rotational coordinate systems that possess solutions to Laplace's equation that are referred to as "R-separable". For simple separability

$$\phi(x_1, x_2) = G(x_1)H(x_2) \tag{3}$$

whereas for "R-separability"

$$\phi(x_1, x_2) = F(x_1, x_2)G(x_1)H(x_2). \tag{4}$$

The tangent–sphere coordinate system is shown in Fig. 2 where it is seen to be comprised of a set of spheres and toroids of various sizes but all

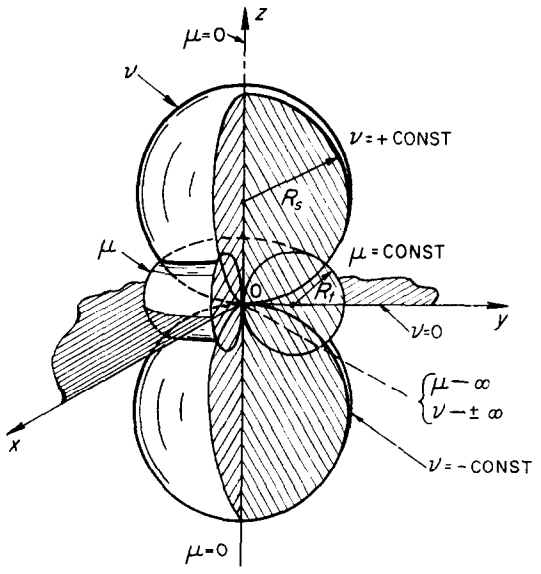

FIG. 2. Tangent–sphere coordinate system.

tangent to a common point which resides in the plane of the solid wall†. Thus, the tangent–sphere coordinate system is seen to be somewhat similar to the more familiar toroidal coordinate system [7]. For convenience, some properties of the tangent–sphere coordinate system are listed as equations (5–10).

$$v = \frac{1}{2R_s} \tag{5}$$

$$\mu = \frac{1}{2R_t} \tag{6}$$

in which R_s is the sphere radius and R_t is the torus radius. The relationship of the v, μ and the r, θ systems is given by

$$\frac{1}{r} = (\mu^2 + v^2)^{\frac{1}{2}} \tag{7}$$

$$\cos\theta = \frac{v}{(\mu^2 + v^2)^{\frac{1}{2}}} \tag{8}$$

† In the present problem we deal only with the positive half space.

$$\mu = \frac{\sin\theta}{r} \tag{9}$$

$$v = \frac{\cos\theta}{r}. \tag{10}$$

In the tangent–sphere coordinate system the axisymmetric form of the Laplacian is

$$\nabla^2\phi = \frac{\partial}{\partial\mu}\left(\frac{\mu}{\mu^2 + v^2}\frac{\partial\phi}{\partial\mu}\right) + \frac{\partial}{\partial v}\left(\frac{\mu}{\mu^2 + v^2}\frac{\partial\phi}{\partial v}\right) \tag{11}$$

and the gradient is

$$\nabla\phi = (\mu^2 + v^2)\left[\frac{\partial\phi}{\partial\mu}\mathbf{i}_\mu + \frac{\partial\phi}{\partial v}\mathbf{i}_v\right] \tag{12}$$

where $\mathbf{i}_\mu$ and $\mathbf{i}_v$ are unit vectors in μ and v directions respectively.

Since $\mathbf{V} = -\operatorname{grad}\phi$, we have the scalar components of velocity;

$$\left.\begin{aligned} V_v &= -(\mu^2 + v^2)\frac{\partial\phi}{\partial v} \\ V_\mu &= -(\mu^2 + v^2)\frac{\partial\phi}{\partial\mu} \\ V_r &= -\frac{1}{(\mu^2 + v^2)^{\frac{1}{2}}}(\mu V_\mu + v V_v) \\ V_\theta &= \frac{1}{(\mu^2 + v^2)^{\frac{1}{2}}}(v V_\mu - \mu V_v) \end{aligned}\right\} \tag{13}$$

where subscripts v, μ, r and θ denote the directions of the components. To generalize our solution we choose the following non-dimensional variables

$$\left.\begin{aligned} v^* &= 2Rv; \qquad \mu^* = 2R\mu; \qquad \phi^* = \frac{\phi}{2R\dot{R}} \\ r^* &= \frac{r}{2R} \\ V_\mu^* &= \frac{V_\mu}{\dot{R}}; \qquad V_v^* = \frac{V_v}{\dot{R}} \\ V_r^* &= \frac{V_r}{\dot{R}}; \qquad V_\theta^* = \frac{V_\theta}{\dot{R}}. \end{aligned}\right\} \quad (14)$$

The surface of the bubble of radius $R(t)$ is located at time t at $v_0 = [1/2R(t)]$ in real space and at $v^* = 1$ in the nondimensional space. The plane wall is at $v^* = 0$. $\mu^* = 0$ represents the axis of symmetry.

In the dimensionless coordinates, Laplace's equation becomes

$$\frac{\partial}{\partial \mu^*}\left[\frac{\mu^*}{\mu^{*2} + v^{*2}}\frac{\partial \phi^*}{\partial \mu^*}\right] + \frac{\partial}{\partial v^*}\left[\frac{\mu^*}{\mu^{*2} + v^{*2}}\frac{\partial \phi^*}{\partial v^*}\right] = 0, \quad (15)$$

$$0 < \mu^* < \infty \qquad 0 < v^* < 1.$$

We seek a solution to (15) subject to boundary conditions.

$$\frac{\partial \phi^*}{\partial \mu^*} = 0, \qquad \mu^* = 0; \qquad 0 \leqslant v^* \leqslant 1 \quad (16a)$$

$$\frac{\partial \phi^*}{\partial v^*} = 0, \qquad v^* = 0; \qquad 0 \leqslant \mu^* < \infty \quad (16b)$$

$$\left.\frac{\partial \phi^*}{\partial v^*}\right|_{v^*=1} = \frac{2}{(\mu^{*2} + 1)^2} \quad (16c)$$

$$\phi^* \to 0, \qquad \left.\begin{matrix} v^* \\ \mu^* \end{matrix}\right\} \to 0. \quad (16d)$$

We note that at the point of tangency ($\mu^* = \infty$, $v^* = 0$), the velocity components V_μ^* and V_v^* are zero on physical grounds which will provide a check on our mathematical formulation.

It is shown by Moon and Spencer [6] that solutions to (15) can be expressed as

$$\phi^*(\mu^*, v^*) = (\mu^{*2} + v^{*2})^{\frac{1}{2}} M(\mu^*)N(v^*) \quad (17)$$

in which M and N are real functions that satisfy the ordinary differential equations

$$\left.\begin{aligned} &\frac{d^2M}{d\mu^{*2}} + \frac{1}{\mu^*}\frac{dM}{d\mu^*} - \alpha M = 0 \\ &\frac{d^2N}{dv^{*2}} + \alpha N = 0 \end{aligned}\right\} \quad (18)$$

and α is a real separation constant which may be either positive, zero or negative. Since the potential is bounded α cannot be positive or zero. When $\alpha = -q^2$ we obtain the desired general solutions to (18).

$$\left.\begin{aligned} M &= A_1 J_0(q\mu^*) + B_1 Y_0(q\mu^*) \\ N &= A_2 \sinh(qv^*) + B_2 \cosh(qv^*) \end{aligned}\right\} \quad (19)$$

Application of the first boundary condition, equation (16a), yields $B_1 = 0$. Equation (16b) gives $A_2 = 0$. Consequently a particular solution is

$$\phi^*(\mu^*, v^*) = A(\mu^{*2} + v^{*2})^{\frac{1}{2}} \times J_0(q\mu^*)\cosh(qv^*) \quad (20)$$

as may be confirmed by substitution into equation (15). It remains to obtain the constant A and the eigenvalues q from the third and fourth boundary conditions. Since we are dealing with a semi-infinite span in μ^* the eigenvalues are continuous and the superposition of solutions therefore requires integration rather than summation. In the present case we propose a solution to the problem in the form

$$\phi^*(\mu^*, v^*) = (\mu^{*2} + v^{*2})^{\frac{1}{2}} \times \int_0^\infty A(q)\, J_0(q\mu^*)\cosh(qv^*)\, dq \quad (21)$$

where $A(q)$ is as yet an unknown function. If now the third boundary condition equation (16c) is invoked

$$\left.\frac{\partial\phi^*}{\partial v^*}\right|_{v^*=1} = \frac{2}{(\mu^{*2}+1)^2}$$

$$= (\mu^{*2}+1)^{\frac{1}{2}} \int_0^\infty A(q) q \sinh q J_0(q\mu^*)\,\mathrm{d}q$$

$$+ \frac{1}{(\mu^{*2}+1)^{\frac{1}{2}}} \int_0^\infty A(q) \cosh q J_0(q\mu^*)\,\mathrm{d}q. \quad (22)$$

The problem of determining $A(q)$ is thus reduced to the solution of this integral equation. To solve the equation for $A(q)$ it is convenient to reduce it in turn to a differential equation. We may write Bessel's equation in the form

$$q\frac{\mathrm{d}}{\mathrm{d}q}\left[q\frac{\mathrm{d}J_0(q\mu^*)}{\mathrm{d}q}\right] + \mu^{*2}q^2 J_0(q\mu^*) = 0 \quad (23)$$

and after rearranging

$$J_0(q\mu^*) = -\frac{1}{\mu^{*2}q}\quad \frac{\mathrm{d}}{\mathrm{d}q}\left[q\frac{\mathrm{d}J_0(q\mu^*)}{\mathrm{d}q}\right]. \quad (24)$$

Rearranging (22) gives

$$\frac{2}{(\mu^{*2}+1)^{\frac{1}{2}}} = \int_0^\infty A(q)\,\mu^{*2} q \sinh q\, J_0(q\mu^*)\,\mathrm{d}q$$

$$+ \int_0^\infty A(q)\,[q\sinh q + \cosh q]\, J_0(q\mu^*)\,\mathrm{d}q$$

$$= I_1 + I_2. \quad (25)$$

Integration of I_1 by parts twice using (24) then yields

$$I_1 = \left[q\sinh q A(q)\frac{\mathrm{d}J_0(q\mu^*)}{\mathrm{d}q}\right]_0^\infty$$

$$- \left[q\frac{\mathrm{d}}{\mathrm{d}q}\{A(q)\sinh q\}\, J_0(q\mu^*)\right]_0^\infty$$

$$+ \int_0^\infty \frac{\mathrm{d}}{\mathrm{d}q}\left[q\frac{\mathrm{d}}{\mathrm{d}q}\{A(q)\sinh q\}\right] J_0(q\mu^*)\,\mathrm{d}q. \quad (26)$$

As can be seen from equation (21) the integral representation for the potential ϕ^* will exist only if the improper integral, containing the function $A(q)$, converges. This requires boundedness conditions on $A(q)$ throughout its domain of definition. In order to insure its behavior at the end points we shall assume here and in the following that $A(q) = 0(q^\alpha)$, $\alpha > 1$, as $q \to 0$ and that $A(q) = 0(q^\beta \mathrm{e}^{-\nu q})$, $\beta < -\frac{1}{2}$, $0 \leqslant \nu \leqslant 1$ as $q \to \infty$. With this, the last remaining boundary condition (16d) is satisfied and $A(q)$ remains bounded with its derivatives for $0 \leqslant q < \infty$. Also the first two terms in equation (26) vanish at both limits and (25) simplifies to

$$F(\mu^*) = \int_0^\infty qK(q)\, J_0(q\mu^*)\,\mathrm{d}q \quad (27)$$

where

$$F(\mu^*) = 2(\mu^{*2}+1)^{-\frac{3}{2}}$$

$$K(q) = \frac{1}{q}\left\{-\frac{\mathrm{d}}{\mathrm{d}q}\left[q\frac{\mathrm{d}}{\mathrm{d}q}\{A(q)\sinh q\}\right] + A(q)\,[q\sinh q + \cosh q]\right\}.$$

The function $F(\mu^*)$ is recognized as the Hankel transform of $K(q)$. Knowing $F(\mu^*)$ the solution of the integral equation is found to be [7]

$$K(q) = 2\,\mathrm{e}^{-q}. \quad (28)$$

There results from equation (27) the second order differential equation for $A(q)$

$$-\frac{\mathrm{d}}{\mathrm{d}q}\left[q\frac{\mathrm{d}}{\mathrm{d}q}\{A(q)\sinh q\}\right] + [q\sinh q + \cosh q]\, A(q) = 2q\,\mathrm{e}^{-q}. \quad (29)$$

By setting

$$B(q) = \frac{\mathrm{d}}{\mathrm{d}q} A(q) \tag{30}$$

one quadrature can be carried out and the equation is reduced to one of first order

$$\frac{\mathrm{d}A(q)}{\mathrm{d}q} = B(q) = \frac{1}{2q \sinh^2 q} \times [C - (q^2 + q\,\mathrm{e}^{-2q} + \tfrac{1}{2}\mathrm{e}^{-2q})] \tag{31}$$

in which C is a constant of integration. It is seen from (31) that $B(q) \to 0$ as $q \to \infty$ independent of C but $B(q)$ diverges as $q \to 0$ unless $C = \frac{1}{2}$. Consequently $C = \frac{1}{2}$ was chosen so the weighting function $A(q)$ will have a bounded derivative at $q = 0$. If one does not insist on this, $A(q) = O(q^{-2})$ as $q \to 0$ instead of the required $O(q^{\alpha})$, $\alpha > -1$, and the integral (21) for the potential ϕ^* diverges. Equation (31) then becomes

$$\frac{\mathrm{d}A(q)}{\mathrm{d}q} = \frac{1}{2q \sinh^2 q} \times [\tfrac{1}{2}(1 - \mathrm{e}^{-2q}) - q^2 - q\,\mathrm{e}^{-2q}]. \tag{32}$$

The equation is rearranged by expanding the exponentials in power series

$$\frac{\mathrm{d}A(q)}{\mathrm{d}q} = -\frac{2q^2}{\sinh^2 q} \sum_{n=0}^{\infty} a_n q^n, \quad q \geqslant 0 \tag{33}$$

where

$$a_n = \frac{(-2)^n}{(n+3)(n+1)!}. \tag{34}$$

If the hyperbolic sine term is also written in series form one obtains

$$-\frac{1}{8}\frac{\mathrm{d}A(q)}{\mathrm{d}q} = \sum_{n=1}^{\infty} m\,\mathrm{e}^{-2mq} \sum_{n=0}^{\infty} a_n q^{n+2}. \tag{35}$$

The double series (35) is absolutely and uniformly convergent in the interval $[0, q]$ thus allowing term-by-term integration. Integrating equation (35) over these limits then gives

$$A(q) - A(0) = \sum_{m=1}^{\infty} \sum_{n=0}^{\infty} \frac{(-1)^n (n+2)}{(n+3)\,m^{n+2}} \times \left\{ \mathrm{e}^{-2mq} \left[\frac{(2mq)^{n+2}}{(n+2)!} + \frac{(2mq)^{n+1}}{(n+1)!} + \ldots + 1 \right] - 1 \right\}. \tag{36}$$

Since $A(q) \to 0$ as $q \to \infty$, it was possible to evaluate equation (36) numerically at large q to obtain $A(0) = 0{\cdot}625$. The exact solution for $A(q)$ is then

$$A(q) = 0{\cdot}625 + \sum_{m=1}^{\infty} \sum_{n=0}^{\infty} \frac{(-1)^n (n+2)}{(n+3)\,m^{n+2}} \times \left\{ \mathrm{e}^{-2mq} \left[\frac{(2mq)^{n+2}}{(n+2)!} + \frac{(2mq)^{n+1}}{(n+1)!} + \ldots + 1 \right] - 1 \right\}. \tag{37}$$

The series was numerically evaluated and the results are shown in Table 1 and on Fig. 3.

Table 1. *Numerical values for weighting function* $A(q)$

q	Approximate solution equation (42)	Exact series solution equation (36)	Numerical integration of equation (32)
0	0·654	0·625	0·630
0·5	0·355	0·356	0·357
1·0	0·186	0·186	0·187
1·5	0·0906	0·0913	0·0921
2·0	0·0475	0·0426	0·0429
3·0	0·00885	0·00823	0·00834
4·0	0·00140	0·00140	0·00143
5·0	0·00026	0·00023	0·00024
6·0	0·00004	0·00002	0·00003

APPROXIMATE SOLUTION

With the exact $A(q)$ found one can, in principle, construct the solution for the potential ϕ^* as given by equation (21). The numerical evaluation

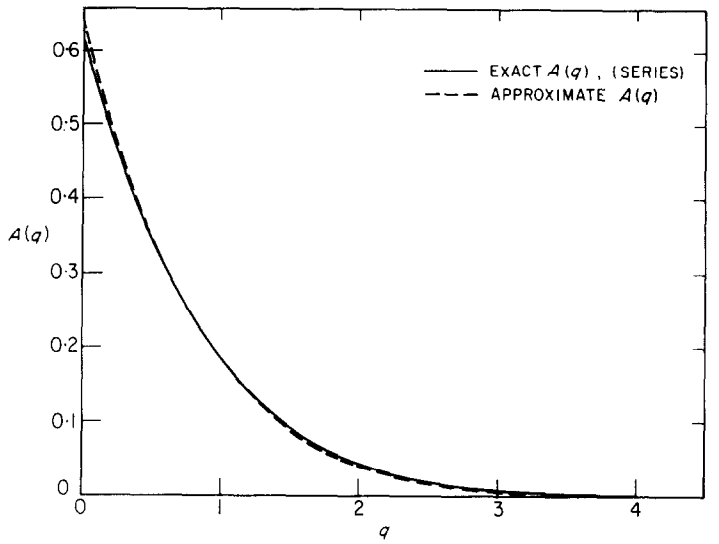

FIG. 3. Comparison of approximate and exact $A(q)$.

of the potential requires an additional integration which appears not reducible to a closed form result. Thus the evaluation of the exact solution was not carried beyond equation (37). Instead a simple analytical approximation was fitted to the known $A(q)$ choosing a form amenable to closed form integration of equation (21). Adequate representation of $A(q)$ was obtained by the sum of terms of the form e^{-aq} and $q e^{-bq}$. These functions are suggested by the form of equation (37) and the following well known integrals exist, i.e. [8]

$$\int_0^\infty e^{-at} J_0(bt)\,dt = \frac{1}{(a^2+b^2)^{\frac{1}{2}}}, \quad \begin{matrix} a>0 \\ b \text{ arbitrary} \end{matrix} \tag{38}$$

and

$$\int_0^\infty t e^{-at} J_0(bt)\,dt = \frac{a}{(a^2+b^2)^{\frac{1}{2}}}, \quad \begin{matrix} a>0 \\ b \text{ arbitrary.} \end{matrix} \tag{39}$$

The solution for the velocity potential may now be written

$$\phi^* = \sum_i A_i \phi_i^* + \sum_j B_j \phi_j^* \tag{40}$$

where

$$\phi_i^* = (\mu^{*2} + \nu^{*2})^{\frac{1}{2}} \int_0^\infty 2 e^{-a_i q} J_0(q\mu^*) \times \cosh(q\nu^*)\,dq \tag{40a}$$

$$\phi_j^* = (\mu^{*2} + \nu^{*2})^{\frac{1}{2}} \int_0^\infty 2 e^{-b_j q} J_0(q\mu^*) \times \cosh(q\nu^*)\,dq. \tag{40b}$$

(The factor of 2 is introduced for later convenience.)

Trial led to the selection of the following set of coefficients:

$$\left.\begin{aligned} A_1 &= 0{\cdot}327, & a_1 &= 1{\cdot}6; \\ B_1 &= 0{\cdot}218, & b_1 &= 2{\cdot}2; \\ B_2 &= 0{\cdot}500, & b_2 &= 2{\cdot}5; \\ B_3 &= -0{\cdot}625, & b_3 &= 2{\cdot}8. \end{aligned}\right\} \tag{41}$$

These coefficients give the approximate result

$$A(q) = 0{\cdot}654 e^{-1{\cdot}6q} + 0{\cdot}436q e^{-2{\cdot}2q} + q e^{-2{\cdot}5q} - 1{\cdot}25q e^{-2{\cdot}8q}. \tag{42}$$

This result is compared with the exact

solution, equation (37), in Fig. 3 where it is seen that the agreement is excellent. Numerical integration of the ordinary differential equation (31) for $A(q)$ was also carried through (using the trapezoidal integration rule) and that result is compared in Table 1 with the exact $A(q)$ calculated from equation (36) and the approximation, equation (42). The exact and numerical results differ by only 0·029 at $q = 0$ and by smaller amounts for other values of q.

Evaluation of the velocity potential from equation (21) using the $A(q)$ given by equation (42) requires integration of the form of equations (40a) and (40b). The results are

$$\phi_i^* = (\mu^{*2} + \nu^{*2})^{\frac{1}{2}} \left\{ \frac{1}{[\mu^{*2} + (b_j - \nu^*)^2]^{\frac{1}{2}}} - \frac{1}{[\mu^{*2} + (b_j + \nu^*)^2]^{\frac{1}{2}}} \right\} \quad (43)$$

and

$$\phi_j^* = (\mu^{*2} + \nu^{*2})^{\frac{1}{2}} \left\{ \frac{(b_j - \nu^*)}{[\mu^{*2} + (b_j - \nu^*)^2]^{\frac{1}{2}}} - \frac{(b_j + \nu^*)}{[\mu^{*2} + (b_j + \nu^*)^2]^{\frac{1}{2}}} \right\}. \quad (44)$$

The velocity components contributed by terms in the potential, equation (40), of the form (43) and (44) are presented for convenience in the Appendix.

Examination of equations (A-7), (A-8), (A-9) and (A-10) reveals that the predicted flow field has the property of approaching spherical symmetry as r^* becomes large, i.e.

$$V_\theta^* \to 0$$

and

$$V_r^* \to \frac{2}{r^{*2}} \left[\frac{A_1}{a_1} + \frac{B_1}{b_1^2} + \frac{B_2}{b_2^2} + \frac{B_3}{b_3^2} \right] \quad \text{as} \quad r^* \to \infty.$$

A standard *uniqueness* theorem [9] for the second boundary value problem of Laplace's equation applied to an infinite region indicates that the solution must satisfy regularity conditions at infinity. More specifically this means that the potential must satisfy

$$|\phi^*| < A/r^*$$

and

$$\left|\frac{\partial \phi^*}{\partial \mu^*}\right| < \frac{A}{r^{*2}}; \qquad \left|\frac{\partial \phi^*}{\partial \nu^*}\right| < \frac{A}{r^{*2}} \qquad \text{as} \quad r^* \to \infty.$$

We now address ourselves to the exact solution equation (21) with the actual kernel replaced by the excellent approximation equation (42). The reader can see now from the above behavior of V_r^* and ϕ^* that our solution meets these criteria.

As a further check on the result the component of velocity normal to the bubble surface was calculated and compared in Fig. 4 with the known boundary condition equation (2c). The agreement is excellent (maximum deviation is about 2 per cent of the maximum velocity). We also note that the constants given by equation (41) give the value of $V_r^* = 0{\cdot}4992/r^{*2}$ at large r^* instead of $V_r^* = \frac{1}{2} \cdot 1/r^{*2}$ as required for spherical symmetry. This shows that the total flow rate is predicted very closely and therefore the small error in the boundary condition on the bubble averages out.

PROPERTIES OF THE FLOW FIELD

The radial velocity component in the $r - \theta$ system of Fig. 1 was calculated throughout the flow field and is presented in Fig. 5 for various values of θ. Also shown is the bubble surface to represent the termination of the curve for each angle. As can be seen this presentation shows the approach to the $1/r^{*2}$ behavior at large r^*.

The streamlines were found and are plotted in Fig. 6 in which one tenth of the total flow is carried by each streamtube. As expected this figure shows that there is relatively little liquid displaced by the growing bubble near the solid wall. Of course there is no flow at the base of the bubble and between $\phi = 143{\cdot}2°$ and 180° only 1 per cent of the total flow is produced. This figure also shows that the flow becomes purely

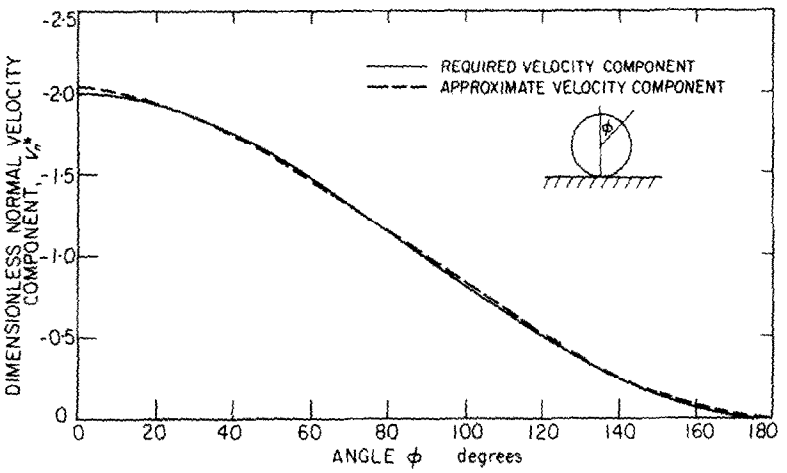

FIG. 4. Comparison of approximate and the required boundary condition, equation (2c).

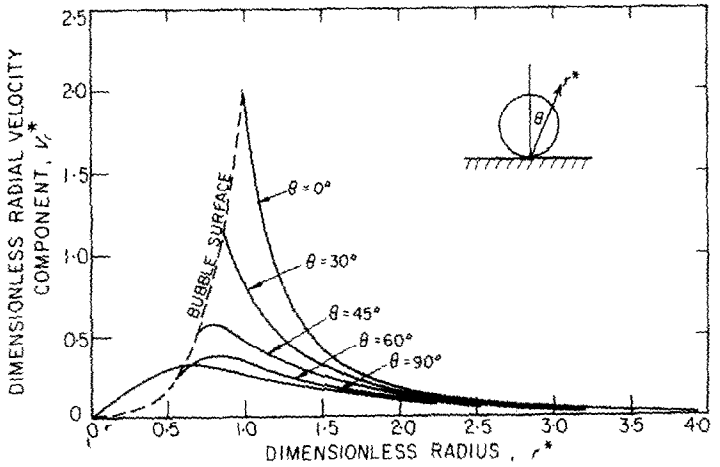

FIG. 5. Radial velocity component.

radial at a distance of about $6R$ from the base of the bubble.

Figure 7 shows the distribution on the bubble surface of the velocity potential and the tangential velocity. Clearly the bubble is not an equipotential surface; the maximum potential occurs on the top of the bubble. The tangential component of liquid velocity on the surface is toward the bottom of the bubble for $0 < \phi < 135°$ and away from the base of the bubble for $135° < \phi < 180°$ going to zero again at $\phi = 180°$.

An important property in certain applications such as cavitation and explosions is the total kinetic energy of the liquid. It is given by [10]

$$T = \frac{\rho_l}{2} \int_A \phi \frac{\partial \phi}{\partial n} dA \tag{45}$$

where the normal derivative on the surface of the liquid is

$$\frac{\partial \phi}{\partial n} = \mathbf{n} \cdot \nabla \phi = V_n.$$

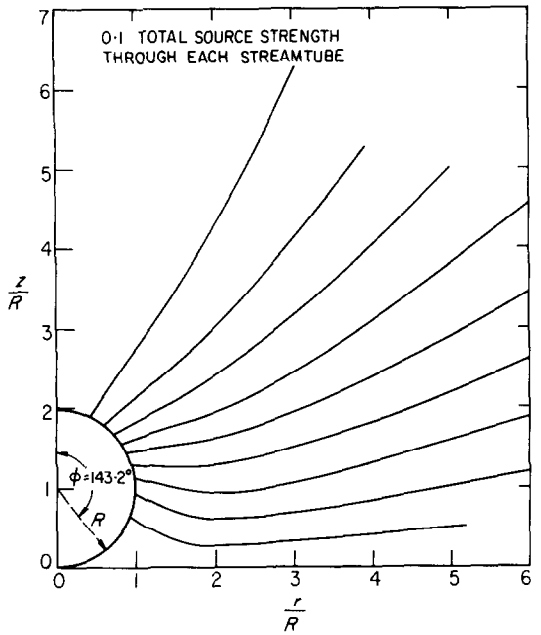

FIG. 6. Streamlines.

With this

$$T = \frac{\rho_l}{2}\int_A \phi(\mu, v_0)\, V_n \, dA. \tag{46}$$

From the geometry

$$V_n = \frac{-2v_0^2\dot{R}}{(\mu^2 + v_0^2)}$$

and

$$dA = \frac{-2\pi\mu\, d\mu}{(\mu^2 + v_0^2)^2}.$$

Defining

$$T^* = \frac{T}{\rho_l \dot{R}^2 R^3} \tag{47}$$

equation (46) can be put into the non-dimensional form

$$T^* = 16\pi \int_{\mu^*=0}^{\mu^*=\infty} \phi^*(\mu^*, 1)\frac{\mu^*\, d\mu^*}{(\mu^{*2} + 1)}. \tag{48}$$

By numerical integration, using Simpson's rule,

$$T^* = 9{\cdot}33$$

A earlier calculation by Shiffman and Friedman [2], in which only the kinetic energy but not the detailed velocity distribution was found, a value of 9·35 was obtained. Thus the two results are in excellent agreement.

With the velocity field known the Bernoulli equation gives the pressure distribution in the liquid. The Bernoulli equation is [10]

$$\tfrac{1}{2}V^2 - \frac{\partial\phi}{\partial t} + \frac{\delta p}{\rho_l} = 0 \tag{49}$$

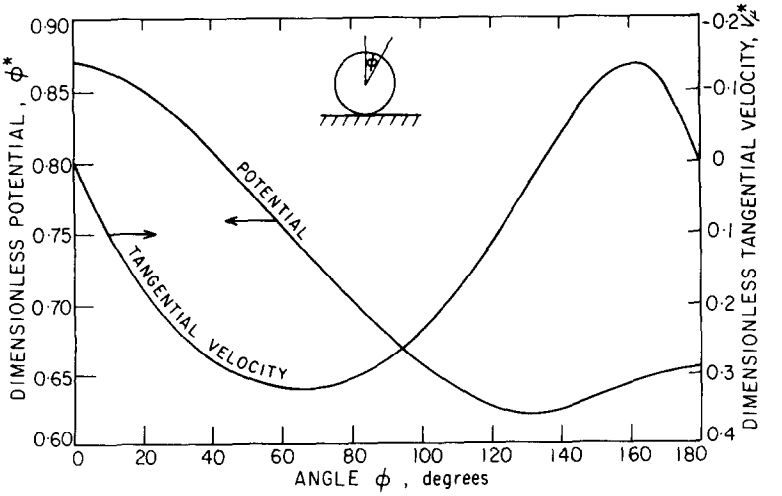

FIG. 7. Flow on bubble surface.

in which

$$\delta p = p(r, \theta) - p(\infty).$$

Also

$$V^2 = \dot{R}^2(V_v^{*2} + V_\mu^{*2}) \tag{50}$$

and

$$\frac{\partial \phi}{\partial t} = \frac{\partial}{\partial t}(2R\dot{R}\phi^*) = 2\phi^*(R\ddot{R} + \dot{R}^2) - 2\dot{R}^2\left(\frac{\mu^* V_\mu^* + v^* V_v^*}{\mu^{*2} + v^{*2}}\right). \tag{51}$$

Choosing, as an example, a bubble growth law of the form $R = \beta t^{\frac{1}{2}}$ we obtain

$$\frac{\delta p}{\rho_l} = -\frac{\beta}{8t}(V_\mu^{*2} + V_v^{*2}) - \frac{\beta^2}{2t}\left(\frac{\mu^* V_\mu^* + v^* V_v^*}{\mu^{*2} + v^{*2}}\right) \tag{52}$$

and on the bubble surface, $v^* = 1$, this reduces to

$$\frac{\delta p t}{\beta^2 \rho_l} = \frac{1}{2}\left(\frac{1}{\mu^{*2} + 1}\right)^2 - \tfrac{1}{8} V_\mu^{*2} - \frac{1}{2}\left(\frac{\mu^* V_\mu^*}{\mu^{*2} + 1}\right). \tag{53}$$

This result is plotted in Fig. 8. The general shape of the pressure distribution is similar to that of the velocity potential. It has a maximum value at the top (north pole) of the bubble at which it is four times as large as in the spherically symmetric case. It decreases with increasing azmuthal angle, ϕ, until reaching zero at about $\varphi = 115°$, then increases again passing through a small maximum at about 150° and finally goes to zero at the base of the bubble where V_μ^*, V_v^* go to zero. This non-monotonic behaviour is associated with the reversal of the tangential component of the liquid velocity at the bubble surface shown in Fig. 7.

The pressure distribution for this idealized geometry (spherical bubble) explains the flattening effect that has been observed for rapidly growing boiling bubbles [11]. For the bubble to retain its spherical shape it is necessary for the inertial pressure in the liquid to be negligible in comparison with the surface tension.

The same force that tends to flatten the bubble also tends to hold the bubble against the wall. For the present model we obtain this force by integrating $\delta p \cos \varphi \, dA$ over the surface of the bubble; the restraining force is

$$F_R = 2\pi \int_0^\pi \delta p \, \beta^2 t \sin \varphi \cos \varphi \, d\varphi. \tag{54}$$

Numerical integration gives with δp expressed

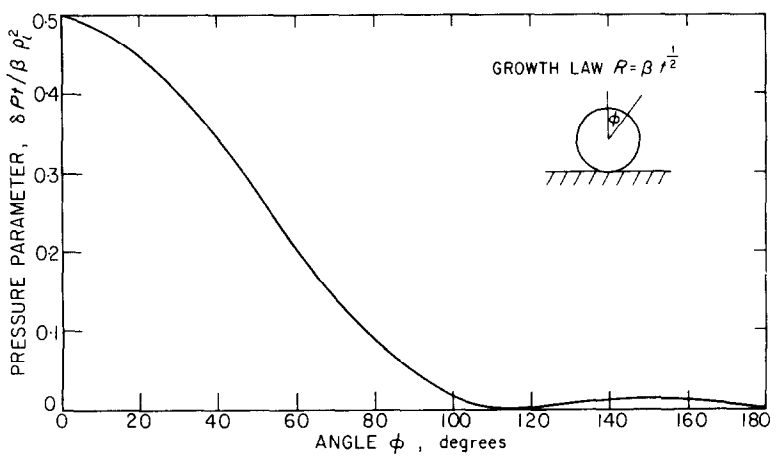

FIG. 8. Pressure distribution on bubble surface.

by equation (53)

$$F_R = 0{\cdot}29\,\pi\beta^4\rho_l. \tag{55}$$

As in the previous calculation the growth law $R = \beta t^{\frac{1}{2}}$ has been adopted. Comparing the restraining force F_R with the buoyant force $F_B = (\rho_l - \rho_g)\frac{4}{3}\pi R^3 g \cong \rho_l \frac{4}{3}\pi R^3 g$ we have

$$\frac{F_R}{F_B} = \frac{0{\cdot}29\,\pi\beta^4\rho_l}{g\frac{4}{3}\pi R^3\rho_g} \cong \frac{3}{16}\frac{\beta}{gt^{\frac{1}{2}}}. \tag{56}$$

Choosing unity for this ratio as a criterion for detachment of bubbles

$$t_d = \left(\frac{3\beta}{16g}\right)^{\frac{1}{2}}. \tag{57}$$

Although this simple calculation neglects surface tension, the more complex shape of real bubbles and is based upon a specific growth law, it does predict departure times that are consistent in magnitude with the saturated boiling experiments of Cole and Shulman [12]. Their results indicate departure times about a factor of three longer suggesting that the factors neglected are important although the restraining force F_R is also important. Several previous investigations have indicated that liquid inertia tends to pull the bubble off the wall and this notion is probably correct. The complexity of bubble shape and its effect on the bubble growth law make a quantitative calculation of this effect very difficult at this time but it seems reasonable that the momentum imparted to the liquid while the bubble is growing rapidly will tend to pull the bubble from the wall after growth has subsided.

Finally it must be stressed that the bubble growth law on which equations (52–57) are based is valid only for asymptotic growth in a spherically symmetric case. For surface boiling of saturated liquid and in some restricted time domains in subcooled boiling this is approximately correct. However for most of the life of bubbles in subcooled boiling there is a serious departure from this growth law. Pressure distributions have not been calculated for other growth laws because the result would probably not be too meaningful. This is because the real bubbles have been observed [11] to undergo major changes in shape that would invalidate the present model. The simple calculations presented here do, however, illustrate the existence of a strong tendency for a rapidly growing bubble to assume a flattened shape. These features are discussed at greater length by Schrock and Perrais [11] and Witze [13].

CONCLUSIONS

The problem of potential flow in a semi-infinite incompressible liquid surrounding a growing spherical cavity tangent to a plane solid surface has been solved. An exact solution for the potential given by equation (21) was found. To obtain a closed form result for the potential and velocity distributions the exact $A(q)$ in equation (21) was approximated by a simple analytical form. This led to a maximum error which occurs on the bubble surface, of only 2 per cent of the maximum velocity.

The solution exhibits the property of approaching purely radial flow at large radial distances from the point of tangency and the magnitude of this flow is in agreement with the volumetric rate of fluid displacement by the growing spherical surface. This consequence of the solution could have been deduced *a priori* on purely physical grounds and was expected.

Other properties of the flow field have been discussed. The total kinetic energy of the fluid, which is of importance in underwater explosions, was calculated from the present result and found to be in close agreement with the earlier result obtained by Shiffman and Friedman. The pressure distribution on the bubble surface was used to develop a criterion for detachment of spherical bubbles from a horizontal surface. This criterion represents physically equality of buoyant force and pressure force. Since the latter depends upon the specific bubble growth law $R(t)$ the resulting equation (57) lacks generality. It is presented here to

emphasize the role of fluid dynamics in the problem of bubble detachment.

The present solution will be useful in studies of boiling bubble dynamics and in cavitation. The problem is an idealization of the true behavior of bubbles, however, since the pressure distribution on the bubble surface will tend to flatten the bubble from the proposed spherical shape. We have used the present result [13] to study certain asymmetric aspects of boiling bubble dynamics according to the asymptotic theory, and the results will be the subject of another paper.

REFERENCES

1. S. KOTAKE, On the mechanism of nucleate boiling, *Int. J. Heat Mass Transfer* **9**, 771 (1966).
2. M. SHIFFMAN and B. FRIEDMAN, On the best location of a mine near a sea bed, *Underwater Explosion Research*, Volume II, U.S. Office of Naval Research (1950).
3. K. FORSTER and N. ZUBER, Growth of a vapor bubble in a superheated liquid, *J. Appl. Phys.* **25**, 474 (1954).
4. G. BIRKHOFF, R. S. MARGULIES, and W. A. HORNING, Spherical bubble growth, *Physics Fluids* **1**, 201 (1958).
5. P. GRIFFITH, Bubble growth rates in boiling, *Trans. Am. Soc. Mech. Engrs* **80**, 721 (1958).
6. P. MOON and D. SPENCER, *Field Theory Handbook*, p. 104. Springer, Berlin (1961).
7. E. HOBSON, *Theory of Spherical and Ellipsoidal Harmonics*, p. 451. Cambridge University Press, Cambridge (1931).
8. G. WATSON, *Theory of Bessel Functions*, p. 384. Cambridge University Press, Cambridge (1944).
9. A. N. TIKHONOV and A. A. SAMARSKII, *Equations of Mathematical Physics*, p. 334. MacMillan, New York (1963).
10. V. STREETER, *Fluid Dynamics*, p. 25. McGraw-Hill, New York (1958).
11. V. E. SCHROCK and J. PERRAIS, Dynamics of bubbles in a known temperature distribution, *Proc.* 1966 *Heat Transf. Fluid Mech. Inst.* paper No. 8, p. 122 (1966).
12. R. COLE and H. SHULMAN, Bubble departure diameters at subatmospheric pressures, *Chem. Engng Prog. Symp. Ser.* **62**, 6 (1966).
13. C. WITZE, The effect of flow and temperature asymmetry on bubble dynamics, Ph.D. Thesis, University of California, Berkeley, California (1967).

APPENDIX

Velocity Components Calculated from the Approximate Solution

The velocity components were obtained from equations (40) through (44) as follows

$$V^*_{v_i} = -(\mu^{*2}+v^{*2})^{\frac{3}{2}}\left\{\frac{(a_i-v^*)}{[\mu^{*2}+(a_i-v^*)^2]^{\frac{3}{2}}} - \frac{(a_i+v^*)}{[\mu^{*2}+(a_i+v^*)^2]^{\frac{3}{2}}}\right\} - v^*(\mu^{*2}+v^{*2})^{\frac{1}{2}}\left\{\frac{1}{[\mu^{*2}+(a_i-v^*)^2]^{\frac{1}{2}}} + \frac{1}{[\mu^{*2}+(a_i+v^*)^2]^{\frac{1}{2}}}\right\} \quad \text{(A-1)}$$

$$V^*_{\mu_i} = -\mu^*(\mu^{*2}+v^{*2})^{\frac{1}{2}}\left\{\frac{1}{[\mu^{*2}+(a_i-v^*)^2]^{\frac{1}{2}}} + \frac{1}{[\mu^{*2}+(a_i+v^*)^2]^{\frac{1}{2}}}\right\} + \mu^*(\mu^{*2}+v^{*2})^{\frac{3}{2}}\left\{\frac{1}{[\mu^{*2}+(a_i-v^*)^2]^{\frac{1}{2}}} + \frac{1}{[\mu^{*2}+(a_i+v^*)^2]^{\frac{1}{2}}}\right\} \quad \text{(A-2)}$$

and

$$V^*_{v_j} = -(\mu^{*2}+v^{*2})^{\frac{3}{2}}\left\{\frac{3(b_j-v^*)^2}{M_-^{\frac{5}{2}}} - M_-^{-\frac{3}{2}} + M_+^{-\frac{3}{2}} - \frac{3(b_j+v^*)^2}{M_+^{\frac{5}{2}}}\right\} - v^*(\mu^{*2}+v^{*2})^{\frac{1}{2}}\left\{\frac{(b_j-v^*)}{M_-^{\frac{3}{2}}} + \frac{(b_j-v^*)}{M_+^{\frac{3}{2}}}\right\} \quad \text{(A-3)}$$

$$V^*_{\mu_j} = -\mu^*(\mu^{*2}+v^{*2})^{\frac{1}{2}}\left\{\frac{(b_j-v^*)}{M_-^{\frac{3}{2}}} + \frac{(b_j+v^*)}{M_+^{\frac{3}{2}}}\right\} + \mu^*(\mu^{*2}+v^{*2})^{\frac{3}{2}}\left\{\frac{3(b_j-v^*)}{M_-^{\frac{5}{2}}} + \frac{3(b_j+v^*)}{M_+^{\frac{5}{2}}}\right\} \quad \text{(A-4)}$$

in which

$$M_+ = \mu^{*2} + (b_j+v^*)^2, \qquad M_- = \mu^{*2} + (b_j-v^*)^2.$$

The complete velocity components are given by

$$V_v^* = A_i V_{v_i}^* + \sum_{j=1}^{3} B_j V_{v_j}^* \qquad \text{(A-5)}$$

and

$$V_\mu^* = A_i V_{\mu_i}^* + \sum_{j=1}^{3} B_j V_{\mu_j}^*. \qquad \text{(A-6)}$$

When transformed to the $r - \theta$ geometry of Fig. 1 the partial velocity components become

$$V_{r_i}^* = \frac{\cos\theta}{r^{*3}}\left\{\frac{\left(a_i - \frac{\cos\theta}{r^*}\right)}{Q_-^{\frac{3}{2}}} - \frac{\left(a_i + \frac{\cos\theta}{r^*}\right)}{Q_+^{\frac{3}{2}}}\right\} + \frac{1}{r^{*2}}\left\{\frac{1}{Q_-^{\frac{1}{2}}} + \frac{1}{Q_+^{\frac{1}{2}}}\right\} - \frac{\sin^2\theta}{r^{*4}}\left\{\frac{1}{Q_-^{\frac{3}{2}}} + \frac{1}{Q_+^{\frac{3}{2}}}\right\} \qquad \text{(A-7)}$$

$$V_{\theta_i}^* = \frac{\sin\theta}{r^{*3}}\left\{\frac{\left(a_i - \frac{\cos\theta}{r^*}\right)}{Q_-^{\frac{3}{2}}} - \frac{\left(a_i + \frac{\cos\theta}{r^*}\right)}{Q_+^{\frac{3}{2}}}\right\} + \frac{\cos\theta\sin\theta}{r^{*4}}\left\{\frac{1}{Q_-^{\frac{3}{2}}} + \frac{1}{Q_+^{\frac{3}{2}}}\right\} \qquad \text{(A-8)}$$

in which

$$Q_+ = \left(\frac{\sin\theta}{r^*}\right)^2 + \left(a_i + \frac{\cos\theta}{r^*}\right)^2$$

$$Q_- = \left(\frac{\sin\theta}{r^*}\right)^2 + \left(a_i - \frac{\cos\theta}{r^*}\right)^2$$

and

$$V_{r_j} = \frac{\cos\theta}{r^{*3}}\left\{\frac{3\left(b_j - \frac{\cos\theta}{r^*}\right)}{T_-^{\frac{5}{2}}} - T_-^{-\frac{3}{2}} + T_+^{-\frac{3}{2}} - \frac{3\left(b_j + \frac{\cos\theta}{r^*}\right)}{T_+^{\frac{5}{2}}}\right\} + \frac{1}{r^{*2}}\left\{\frac{\left(b_j - \frac{\cos\theta}{r^*}\right)}{T_-^{\frac{3}{2}}} + \frac{\left(b_j + \frac{\cos\theta}{r^*}\right)}{T_+^{\frac{3}{2}}}\right\} - \frac{\sin^2\theta}{r^{*4}}\left\{\frac{3\left(b_j - \frac{\cos\theta}{r^*}\right)}{T_-^{\frac{5}{2}}} + \frac{3\left(b_j + \frac{\cos\theta}{r^*}\right)}{T_+^{\frac{5}{2}}}\right\} \qquad \text{(A-9)}$$

$$V_{\theta_j}^* = \frac{\sin\theta}{r^{*3}}\left\{\frac{3\left(b_j - \frac{\cos\theta}{r^*}\right)^2}{T_-^{\frac{5}{2}}} - T_-^{-\frac{3}{2}} + T_+^{-\frac{3}{2}} - \frac{3\left(b_j + \frac{\cos\theta}{r^*}\right)^2}{T_+^{\frac{5}{2}}}\right\} + \frac{\cos\theta\sin\theta}{r^{*4}}\left\{\frac{3\left(b_j - \frac{\cos\theta}{r^*}\right)}{T_-^{\frac{5}{2}}} + \frac{3\left(b_j + \frac{\cos\theta}{r^*}\right)}{T_+^{\frac{5}{2}}}\right\} \qquad \text{(A-10)}$$

in which

$$T_+ = \left(\frac{\sin\theta}{r^*}\right)^2 + \left(b_j + \frac{\cos\theta}{r^*}\right)^2$$

$$T_- = \left(\frac{\sin\theta}{r^*}\right)^2 + \left(b_j - \frac{\cos\theta}{r^*}\right)^2$$

and again the complete velocity components are given by

$$V_r^* = A_i V_{r_i}^* + \sum_{j=1}^{3} B_j V_{r_j}^* \qquad \text{(A-11)}$$

$$V_\theta^* = A_i V_{\theta_i}^* + \sum_{j=1}^{3} B_j V_{\theta_j}^*. \qquad \text{(A-12)}$$

Résumé—On présente une solution décrivant la configuration de l'écoulement potential dans un liquide semi-infini entourant une sphère qui croft tout en restant tangente à une surface solide plane. On donne une représentation intégrale exacte dc la solution pour la distribution du potentiel. Une représentation analytique simple pour l'intégrand a été choisie pour remplacer la forme exacte et fournir ainsi des résultats sous forme analytique à la fois pour la distribution du potentiel et de la vitesse.

Les propriétés du champ d'écoulement sont examinées. L'énergie cinétique totale du fluide est en bon accord avec les résultats d'un calcul plus ancien mais moins détaillé de Shiffman et Friedmann. La distribution de pression a été évaluée pour une loi spécifique de croissance et employée à la formation d'un nouveau critère pour le détachement de la sphère de la surface. La solution devrait trouver des applications dans la dynamique des bulles au cours de l'ébullition, les explosions sous-marines et les études de la cavitation.

Zusammenfassung—Es wird eine Lösung angegeben für das Potentialströmungsfeld in einer halbunendlich ausgedehnten Flüssigkeit, die eine wachsende Kugel umgibt, welche an einer ebenen festen Oberfläche haftet. Eine exakte Integraldarstellung der Lösung für die Potentialverteilung ist angegeben. Eine einfache analytische Darstellung für den Integranden wurde gewählt, um die exakte Form zu ersetzen und dadurch analytische Ergebnisse in geschlossener Form für die Potentialund Geschwindigkeitsverteilung zu erhalten.

Eigenschaften des Strömungsfeldes werden geprüft. Die gesamtkinetische Energie des Mediums stimmt gut mit den Ergebnissen einer früheren aber weniger ins einzelne gehenden Berechnung von Shiffmann und Friedmann überein. Für ein spezifisches Wachstumsgesetz wirde die Druckverteilung ausgewertet und dazu verwendet, ein neues Kriterium für die Ablösung der Kugel von der Oberfläche aufzustellen. Die Lösung lässt sich anwenden in der Dynamik der Siedeblasen, Unterwasserexplosionen und Kavitationsuntersuchungen.

Аннотация—Приводится решение для потенциального обтекания раздувающегося шара, касающегося плоской поверхности твердого тела, полуограниченной жидкостью. Дается точное решение в интегральной форме для потенциального распределения. Выбирается вместо точной простая аналитическая формула подинтегрального выражения для получения в закмнутом виде теоретического распределения потенциала и скорости.

Изучаются свойства полей потока. Данные по общей кинетической энергии жидкости хорошо согласуются с ранее полученными, но менее точными расчетами Шиффмана и Фридмана. В частном случае определяется распределение давления, которое используется для получения нового критерия, описывающего отрыв шара от поверхности. Решение должно найти применение при изучении динамики пузырькового кипения, подводных взрывов и кавитации.